Bioresource Technology 372 (2023) 128632

Contents lists available at ScienceDirect

Bioresource Technology

journal homepage: www.elsevier.com/locate/biortech

Magnetite-based nanoparticles and nanocomposites for recovery of overloaded anaerobic digesters

Raquel Barrena [a,*], María del Carmen Vargas-García [b], Paula Catacora-Padilla [a], Teresa Gea [a], Ahmad Abo Markeb [a], Javier Moral-Vico [a], Antoni Sánchez [a], Xavier Font [a], Thomas J. Aspray [c,d]

[a] GICOM Research Group Department of Chemical, Biological and Environmental Engineering, Universitat Autònoma de Barcelona Edifici Q, Carrer de les Sitges 08193 Bellaterra (Cerdanyola del Vallès), Barcelona, Spain
[b] Department of Biology and Geology, CITE II-B Universidad de Almería CEIMAR Marine Campus of International Excellence, 04120 Almería, Spain
[c] School of Energy, Geoscience, Infrastructure and Society, Heriot-Watt University, Edinburgh EH14 4AS, Scotland, UK
[d] Solidsense Ltd, Bearsden, East Dunbartonshire G61 3BA, Scotland, UK

HIGHLIGHTS

- Iron-based nanomaterials were tested in anaerobic granular and flocculated sludge.
- Magnetite-based nanomaterials were able to recover overloaded anaerobic reactors.
- VFA inhibition were reversed in 30–50 days using nanomaterials.
- Microbiome in granular and flocculated sludge were reestablished with modifications.
- Promoted microorganisms changed the dominance towards hydrogenotrophic species.

GRAPHICAL ABSTRACT

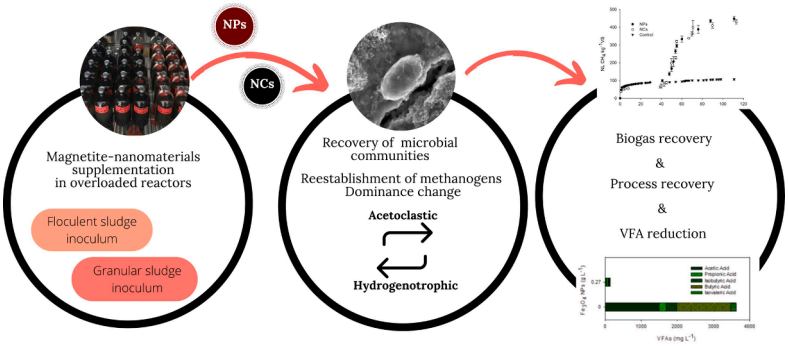

ARTICLE INFO

Keywords:
Iron-oxide nanoparticles
Granular sludge
Flocculent sludge
Hydrogenotrophic methanogens
VFA inhibition

ABSTRACT

The effect of magnetite nanoparticles and nanocomposites (magnetite nanoparticles impregnated into graphene oxide) supplement on the recovery of overloaded laboratory batch anaerobic reactors was assessed using two types of starting inoculum: anaerobic granular sludge (GS) and flocculent sludge (FS). Both nanomaterials recovered methane production at a dose of 0.27 g/L within 40 days in GS. Four doses of magnetite nanoparticles from 0.075 to 1 g/L recovered the process in FS systems between 30 and 50 days relaying on the dose. The presence of nanomaterials helped to reverse the effect of volatile fatty acids inhibition and enabled microbial communities to recover but also favoured the development of certain microorganisms over others. In GS reactors, the methanogenic population changed from being mostly acetoclastic (*Methanothrix soehngenii)* to being dominated by hydrogenotrophic species (*Methanobacterium beijingense)*. Nanomaterial amendment may serve as a preventative measure or provide an effective remedial solution for system recovery following overloading.

* Corresponding author.
E-mail address: raquel.barrena@uab.cat (R. Barrena).

https://doi.org/10.1016/j.biortech.2023.128632
Received 18 November 2022; Received in revised form 12 January 2023; Accepted 13 January 2023
Available online 16 January 2023

1. Introduction

Anaerobic digestion (AD) is a well-established resource recovery technology used commercially around the world. This is especially the case in Europe where AD is playing an increasingly crucial role in the energy transition, diversifying the energy mix with renewable energy sources (Commission and Communication, 2021). Despite its potential, many industrial plants do not operate to their maximum capacity in order to avoid operational problems. For example, operational instability due to fluctuations in organic loading is a common issue. High organic loading rates (OLR) and high content of easily biodegradable substrates can lead to rapid acidification and accumulation of intermediate volatile fatty acids (VFA). The monitoring of VFA to prevent accumulation in anaerobic digesters is a fairly standard practice.

The use of conductive iron oxides, particularly magnetite, has been reported as a strategy to enhance the methanogenic degradation of VFA (digestion intermediates) under ammonia stressed conditions (Lee et al., 2019) leading to an increase in methane production. For example, Baek et al. (2017) found that the addition of magnetite (particle size 100–700 nm) resulted in a more resistant and resilient operation to process imbalances, especially effective in avoiding propionic acid accumulation. The enhanced biomethanation was attributed to the facilitated direct interspecies electron transfer (DIET) between the acetogens and methanogens. DIET between syntrophic microbes associated directly with the anaerobic degradation of VFA were also reported by Yan et al. (2017) using conductive materials. The use of magnetite nanoparticles (NPs) has also been associated with an increase in both VFA formation and subsequent degradation. Zhang et al. (2020) reported a 2.5-fold increase in the formation of VFA and an enhancement in acetoclastic methanogenesis when 100 mg/L of magnetite was used.

In general, the use of conductive additives has been proven to be effective in improving AD performance promoting DIET (Zhang et al., 2018). Of the conductive additives tested to date, graphene has been shown to cause higher electron transfer efficiency in DIET because of its higher conductivity and smaller size than other carbon-based conductive materials (Zhang et al., 2018). Other novel materials with electron donating capacities such as biochar are currently being investigated with promising initial results (Sun et al., 2022).

The effect of the incorporation of NPs in the biochemical aspects of the process has been related to the affectation of the microbiome among other reasons (Wang et al., 2021). Several factors of the AD process have been investigated in terms of their influence on the microbial community (Kong et al., 2018). The relative abundance of methanogens, their composition in terms of acetogenic and hydrogenotrophic species, and the presence of syntrophic bacteria, are basic aspects in the control of AD. It has been shown that the microbial community structure can change depending on the presence and characteristics of the NPs, favouring an increase or decrease in the diversity of both eubacteria and archaea (Wang et al., 2021). In the case of magnetite, the results point to low toxicity, mainly due to the stimulating effect of the presence of Fe^{2+}/Fe^{3+} ions on microbial activity (Arif et al., 2018) that promote DIET. Ma et al. (2021) analysed the changes in microbial community dynamics and found that magnetite caused different syntrophic interactions depending on the OLR. However, this effect may be regulated by the concentration of NPs added (Salama et al., 2021).

Besides the properties of the NPs, the use of different starting inocula can influence the response of the various microbial communities present in the process; however, this has been scarcely studied. Studies have found greater process stability in prokaryotic populations associated with aerobic granular sludge than of flocculent activated sludge, which translates into a lower affectation of biochemical and metabolic events (Daraei et al., 2019). Moreover, the composition of the initial microbiome is already different between GS and FS (De Vrieze et al., 2015). The potential effect of NPs on the different microbiome has not been yet compared. Therefore, there are studies that report the influence on AD of either the incorporation of magnetite NPs or the use of different types of inocula, which provide different microbial communities. However, to our knowledge, studies that merge both factors together do not exist. For this reason, the aim of this work was to study the influence of the type of inoculum in the recovery of overloaded reactors when magnetite-based NPs are added. Two different type of starting inoculum, granular sludge (GS) and flocculent sludge (FS), commonly used in suspended and immobilised biomass of AD, were used and the shift in microbial communities assessed. Instead of commercial magnetite NPs, we carefully synthesized the NPs and characterized their size distribution. Simple magnetite NPs were compared with magnetite NPs impregnated into graphene oxide due to the promising effects of this material previously described. The improvement in VFA removal efficiency could be a significant factor to enhance process stability. This, coupled with an increase in methane yield when using iron-based nanomaterials, opens a new strategy to have a 'doubling effect' when working at high OLR.

2. Materials and methods

2.1. Synthesis and characterization of nanoparticles

Magnetite NPs were synthesized by the coprecipitation method using tetramethylammonium hydroxide (TMAOH) with slight modifications (Abo Markeb et al. 2019). TMAOH was used to increase the colloidal stability of the NPs as well as improve the degree of crystallinity. Briefly, 40 mmol of iron (III) chloride hexahydrate ($FeCl_3{\cdot}6H_2O$), and 20 mmol of iron (II) chloride ($FeCl_2$) were dissolved in 200 mL of deoxygenated water for 20 min. The iron salts solution mixture was added dropwise into 200 mL of 1 M deoxygenated TMAOH at room temperature until the colour of the suspension changed to black. After this, the mixture suspension was vigorously stirred (600 rpm) for 30 min under an inert nitrogen gas stream. Lastly, the Fe_3O_4 NPs were washed three times using magnetic decantation and then redissolved into 1 mM of TMAOH to obtain the final suspension of Fe_3O_4 NPs.

The magnetite nanoparticles impregnated into graphene oxide, Fe_3O_4-rGO nanocomposites (NCs), were prepared in two steps. Reduced graphene oxide (rGO) was prepared in the first step as follows: 1 g of graphite powder was mixed with 0.5 g of sodium nitrate in 23 mL of H_2SO_4 in an ice bath. Then, 3 g of potassium permanganate ($KMnO_4$) was added dropwise after the mixture was stirred for 30 min. Next, the mixture solution was continuously stirred for 4 h in an ice bath (<10 ℃). Afterwards, the reaction was terminated by the addition of 4 mL of H_2O_2, and 146 mL of deionized water. Hence, the graphene oxide produced was separated by centrifugation at 9000 rpm for 20 min, followed by washing with HCl (0.01 M), and deionized water. Lastly, the graphene oxide (GO) was dried at 60 ℃ for 24 h. Next, 0.5 g of the dried GO was dispersed in 100 mL of deionized water by ultrasonication for 2 h. Next, 2 mL of ascorbic acid solution (2.2 mM) was added dropwise into the GO suspension. The resulting rGO was washed three times with deionized water by centrifugation at 9000 rpm for 20 min, followed by drying at 60 ℃ for 24 h. In the second step, magnetite nanoparticles coated with cetyltrimethylammonium bromide (CTAB) were synthesized in presence of the previously described rGO in order to obtain Fe_3O_4 NPs impregnated into rGO by using the in-situ co-precipitation slightly modified method of the previously reported study (Abo Markeb et al., 2019). Briefly, $FeCl_2{\cdot}4H_2O$ (25 mM) and $FeCl_3{\cdot}6H_2O$ (50 mM) in 1:2 M ratio of Fe^{2+}/Fe^{3+}, were dissolved in pre-sonicated and deoxygenated 100 mL of ultrapure water (Milli-Q) containing 0.1 g of CTAB, 0.1 g of rGO. Then, the mixture solution was incubated for 1 h at 40 °C under inter atmosphere by purging with nitrogen. Next, 0.6 M of NH_4OH solution, previously purged with N_2 for 1 h, was added dropwise into the mixed solution under agitation and nitrogen atmosphere until a pH of 9.0 was achieved. During the titration process, the black colour confirmed the formation of Fe_3O_4 NPs. Then, the Fe_3O_4-rGO NCs suspension was stirred continuously under a nitrogen atmosphere for 1 h at 40 °C. Afterwards, the NPs were washed three times using ultrapure water followed by ethanol using magnetic a neodymium magnet and,

then dried at 60 °C for 12 h.

The synthesized nanomaterials were characterized in terms of size, distribution and morphology using a Zeiss Merlin Scanning Electron Microscope (SEM) and using a JEM-2011/JEOL, High-Resolution Transmission Electron Microscope (HR-TEM) equipped with Energy-Dispersive Spectroscopy (EDS). Besides, selected areas electron diffraction images (SAED) were used to study the microstructure of the material with high resolution images. ImageJ free software was used to obtain the size distribution histogram of magnetic NPs from TEM images.

2.2. Inoculum source

Two types of different mesophilic inoculum from full-scale mesophilic anaerobic digesters were used in batch experiments: anaerobic granular sludge (GS) obtained from an up-flow anaerobic sludge blanket (UASB) digester treating wastewater of a local whisky distillery in Edinburgh (Scotland, UK); and anaerobic flocculent sludge (FS) from the mesophilic anaerobic digester of *Riu Sec* municipal wastewater treatment plant (WWTP) (Sabadell, Barcelona, Spain). The total solids (TS) content and volatile solids (VS) content of GS were 3.30 ± 0.01 % and 70.1 ± 0.1 %, respectively, while for FS were 2.70 ± 0.06 % and 64.11 ± 0.08 %, respectively.

2.3. Anaerobic digestion (AD) batch experimental set-up and procedure

Biochemical methane potential (BMP) tests were conducted using glass serum bottles (250 mL) containing inoculum and glucose with/without magnetite-based NPs. The volume of liquid was adjusted in all bottles with water as necessary. pH was adjusted to ~8.0 using 0.1 mL of citric acid (300 g/L) as appropriate. Glucose was added in sufficient amount to inhibit methanogenesis and induce acidification. The inoculum to substrate ratio (ISR) of 2:1 based on vS content was enough to obtain the inhibitory conditions in GS (6.4 g/L). For FS, a higher amount of glucose was needed to inhibit the process and an ISR of 1:1 was required (21.3 g/L). Previous experiments showed that these concentrations were suitable for sustained inhibition of the complete AD process. The headspace of each bottle was purged with nitrogen gas for one minute to ensure anaerobic conditions. The bottles were incubated at 37 °C with continuous mixing for experiments using GS (orbital incubator, 110 rpm) and intermittent mixing (turn up down twice/three times a week) for FS.

Blank assays containing inoculum without glucose were used to subtract the background methane production from the inocula. Positive controls using microcrystalline cellulose were also established to validate inocula activity (Holliger et al., 2016). Each experiment treatment/control was setup in triplicate as a minimum. For GS, Fe_3O_4 NPs and Fe_3O_4-rGO NCs were added to glucose-fed reactors in a concentration of 0.27 g/L as previously used by the same authors (Casals et al., 2014). BMP of TMAOH at the same concentration as the final suspension of Fe_3O_4 NPs was also evaluated in glucose-fed reactors to discard any effect of this additive on the process. For FS, four doses of magnetite NPs from 0.075 to 1 g/L were tested in glucose-fed reactors. The experiments were carried out for at least 100 days irrespective of inoculum type.

2.4. Analytical methods

TS and vS content and pH were determined according to standard methods. VFA samples were analysed by high-pressure liquid chromatography-ultraviolet detection after filtering (0.22 μm) as previously described in Barrena et al. (2021). Biogas composition was analysed by gas chromatography as described in Casals et al. (2014).

2.5. Microbial community analysis

Sequencing and bioinformatics were performed by Life Sequencing S.A. (Valencia, Spain). PowerSoil™ DNA Isolation kit (MoBio Laboratories Inc., Carlsbad, CA, USA) was used for the extraction of DNA as per the manufacturers' instructions. Sequencing data obtained from the Illumina MiSeq platform (Illumina, Ic., San Diego, CA, USA) were analysed according to our previous works (Barrena et al., 2021).

2.6. Statistical analysis

Statistical analysis was based on one-way ANOVA ($p < 0.05$ confidence) with the Tukey test. Significant differences were analysed using Minitab 16 (Minitab Inc.). The alpha diversity indices of the different microbial communities were obtained from the EzBioCloud microbiological research platform (https://www.ezbiocloud.net), while the SIMPER and Indicator Species analyses, as well as the dendrogram, were performed using the PAST software for statistical analysis of biological data (PAST 4.05). The phylogenetic tree showing the evolutionary relationship of the dominant amplicon sequence variants (ASVs) was generated from MEGA version 10.1.6 software, using the Neighbour-Joining method combined with the Maximum Composite Likelihood method to compute evolutionary distances.

3. Results and discussion

3.1. Nanomaterials characterisation

The size of synthesised magnetite ranged from 6 to 13 nm, with 60 % falling between 8 and 10 nm (Fig. 1A, B). As seen in Fig. 1D and 1E the synthetized materials are highly crystalline in nature. In particular, Fig. 1C shows a high-resolution TEM image in which crystalline planes of a single nanoparticle are clearly described, which is confirmed by the SAED image of Fig. 1E, where the typically reported pattern for magnetite can be distinguished (Cai and Wan, 2007). This pattern was less clear when NPs are analysed in a sample taken from the anaerobic digester (Fig. 1F) assumed due to the presence of inoculum and substrate.

The presence of graphene cannot be confirmed with this analysis due to its amorphous structure, but as observed in Fig. 1C, the impregnation of NPs with rGO causes the image of NPs not to be as clear as non-impregnated NPs (Fig. 1A) and new structures corresponding to graphene oxide appear. SEM images were analysed to determine the interaction established between nanomaterials and inoculum (see supplementary material).

3.2. Recovery of overloaded batch reactors inoculated with granular sludge (GS)

The specific methane production in the experiment using GS is shown in Fig. 2A. As expected, the amount of glucose added to the reactor was enough to inhibit the process. Methane content in biogas was <30 %, suggesting the inhibition of methanogenic microorganisms. Low methane content was maintained during all the process in control reactors with glucose. However, as observed in Fig. 2A, reactors supplemented with magnetite NPs recovered from the inhibition after 40 days. The specific methane production rose and the concentration of methane in biogas increased to 60–65 %. Even though this is a significant period in a discontinuous digestion, these results are encouraging as per the implications of the use on NPs or NCs at a commercial scale. This suggests the hypothesis that a continuous digester microbiome adapted to the presence of NPs would potentially have the ability to overcome drastic changes in OLR without the need of long adaptation periods, to be confirmed in future experiments.

Fig. 2B shows VFA content in reactors 45 days after NP supplementation and comparative controls. As observed, the total VFA in control reactors was 3100 mg/L, almost entirely composed of acetic and butyric acid (each 1500 mg/L), and more than double the threshold (1500 mg/L total VFA) considered to guarantee a stable digestion process

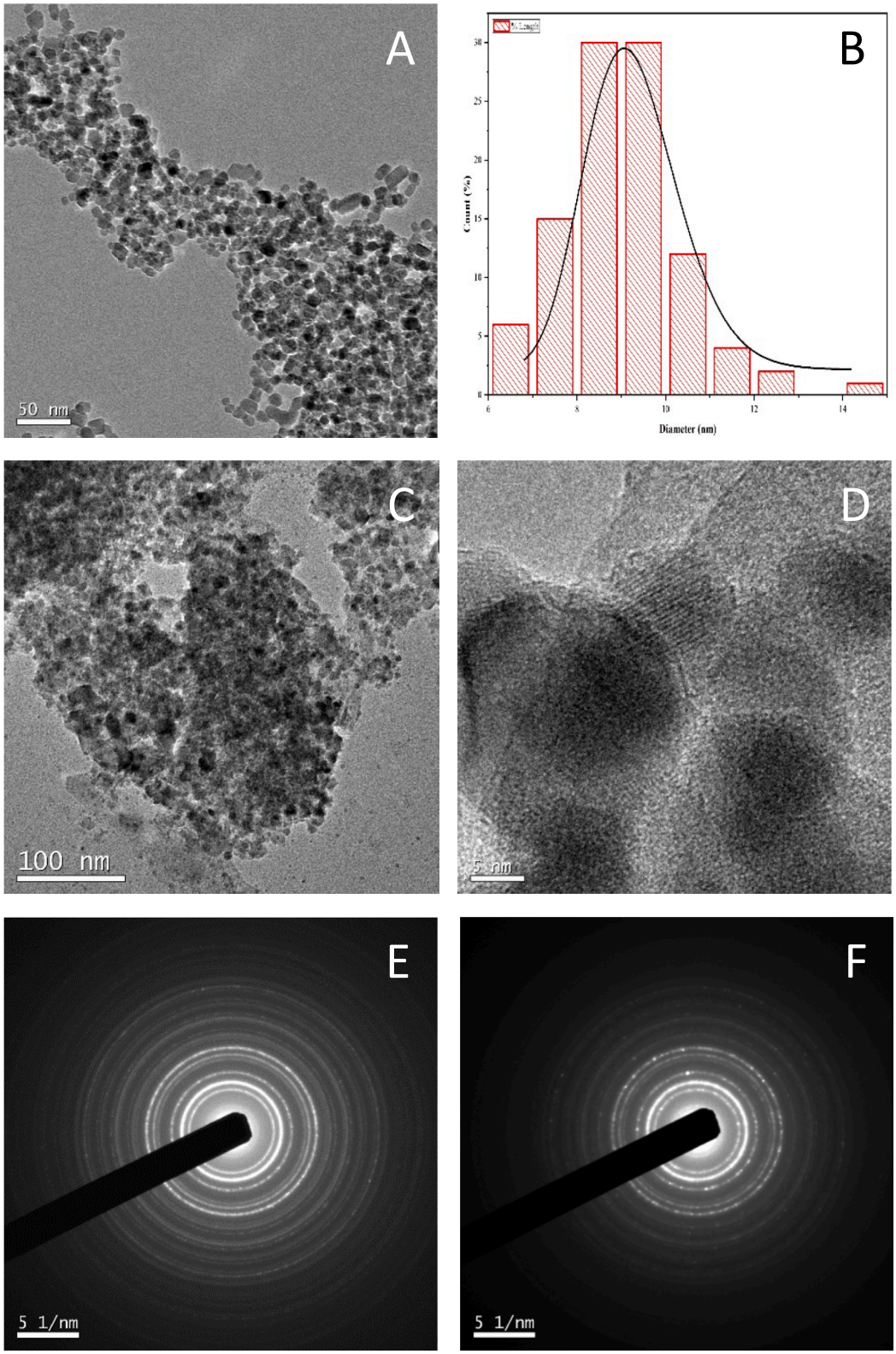

Fig. 1. Nanoparticles characterisation: TEM images: A) magnetite nanoparticles, B) distribution size histogram of magnetite NPs obtained from TEM images, C) Magnetite NPs impregnated with rGO, D) high resolution image of magnetite nanoparticles, E) SAED pattern of magnetite nanoparticles, F) SAED pattern of magnetite nanoparticles after being added to an anaerobic digester.

(Angelidaki et al., 2005). Siegert and Banks (2005) reported that fermentation of glucose was inhibited at VFA concentrations above 4000 mg/L. The accumulation of VFA is thought to explain the failure of control reactors. They presented a very low methane production (around 100 NL methane kg^{-1} VS) being clearly affected by the inhibitory conditions. No signs of recovery were observed for more than 100 days. In contrast, the recovery of supplemented reactors was accompanied by the reduction of total VFA, presenting a total amount lower than 80 mg/L

A)

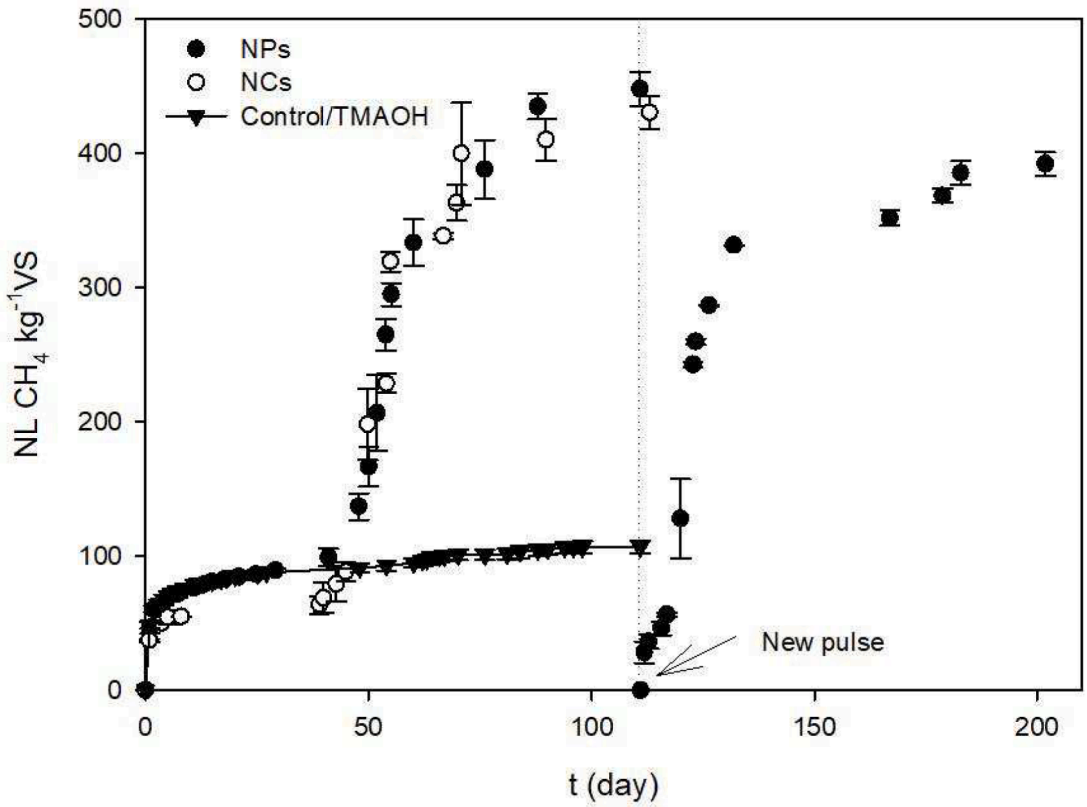

B)

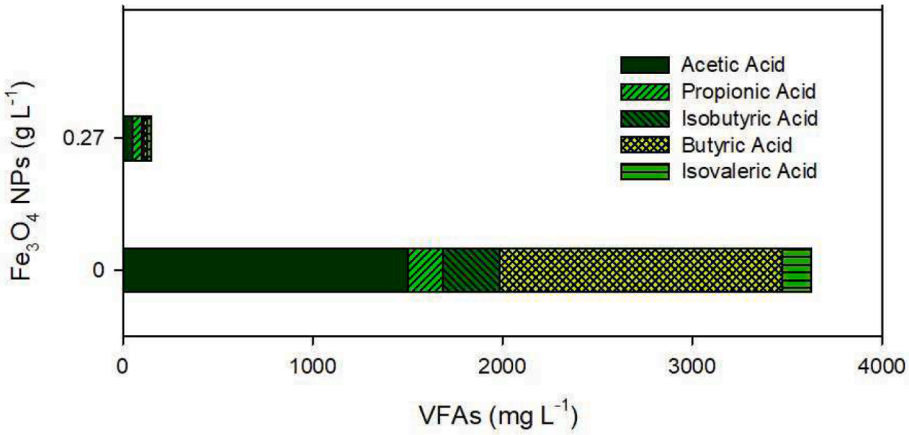

Fig. 2. A) Evolution of methane production of overloaded reactors with and without iron-based NPs (NPs and NCs) at a dose of 0.27 g/L in granular sludge; B) Volatile fatty acid (VFA) content (mg/L) after the recovery of reactors supplemented with NPs.

(Fig. 2B). After the recovery, reactors with NPs presented a specific methane production close to the theoretical production for a carbohydrate (415 NL methane kg^{-1}VS).

The methane production profile obtained in the reactors supplemented with NCs is also shown in Fig. 3a. As observed, the addition of NCs had a similar effect to that of the NPs in the recovery of methanogenesis. Other authors pointed out differences in the effects of using the same type of NPs and NCs in biological processes. For instance, Sun et al. (2021) observed that both nanomaterials could intensify butyrate-type fermentation and other positive aspects in dark fermentation, but the enhancement effect of Fe_3O_4-rGO NCs was superior. Concerning the recovery of the AD systems studied in this work, no significant differences were observed for time recovery or methane production. Thus, the addition of graphene did not improve the effect of magnetite NPs confirming the potential use of this more simple and lower cost material. The microbiological study confirmed these minimal differences between NCs and NPs (see section 3.4). To author's knowledge, the effect of NCs on the anaerobic digestion performance has been scarcely studied and it is interesting to have new data for further applications.

Methane production of the assay containing TMAOH (1 mM) did not

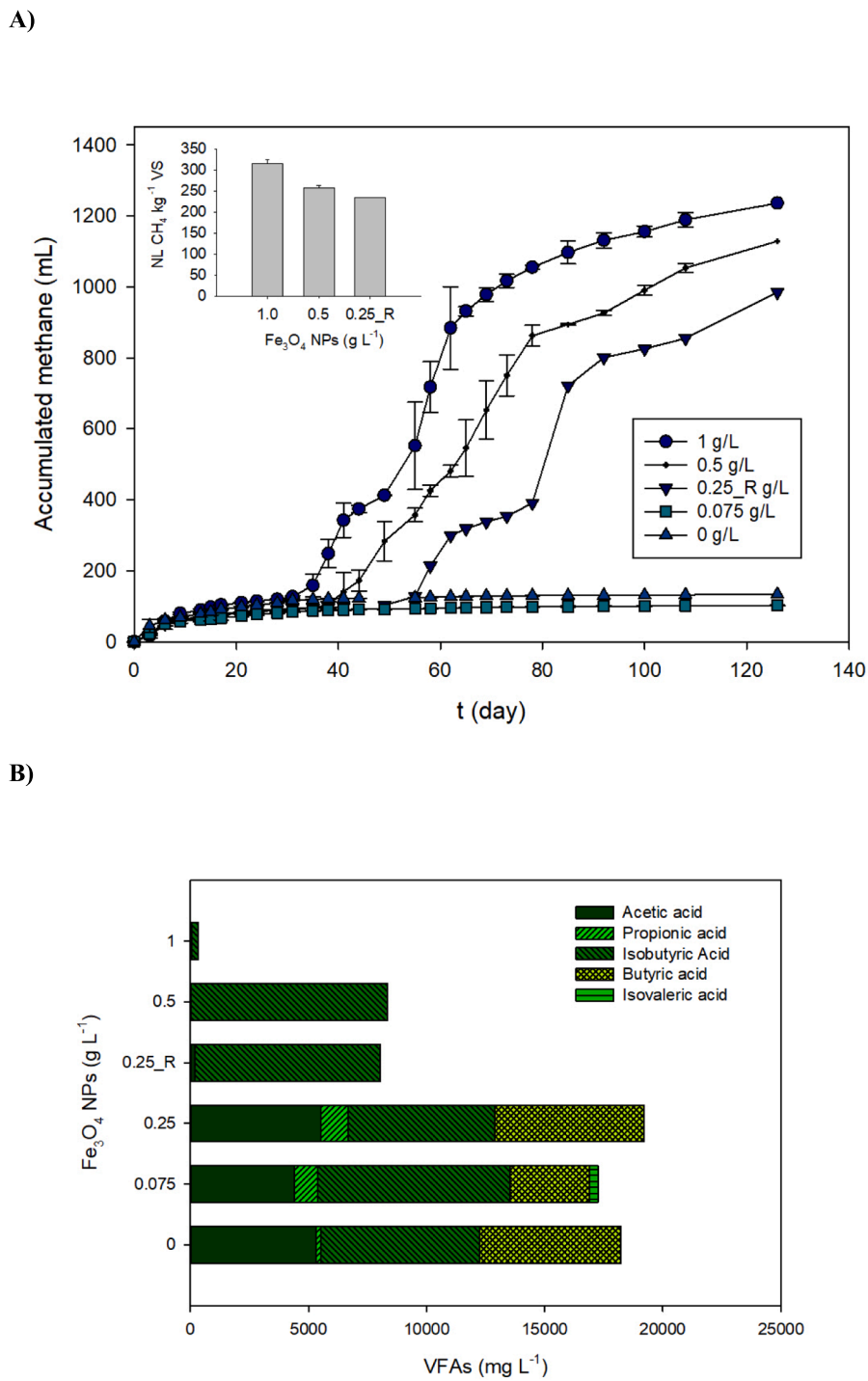

Fig. 3. A) Evolution of methane production of overloaded reactors with and without NPs at different doses in flocculent sludge; B) Volatile fatty acid (VFA) content (mg/L) after the recovery of reactors supplemented with NPs.

show any differences in methane production in comparison with the control (Fig. 2A). The process did not recover over the time the test was carried out (100 days). The effect of stabilizers used in NPs synthesis is not usually described in works dealing with magnetite NPs and AD. However, it has been previously reported that TMAOH could be anaerobically degraded (Whang et al., 2014), which could imply an increase in biogas production or also present other side effects. However, to discount other effects of TMAOH, the microbial community of these bioreactors were also analysed and compared with other samples as described below (section 3.4).

After 100 days of process, NPs and NCs were added to glucose inhibited reactors (data not shown). Interestingly, when NPs and NCs were added, anaerobic digesters recovered from failure within 40 days, the same time observed in all previously recovered processes (Fig. 2A). As no difference was observed between supplementing the magnetite-based NPs at the start or during the test, the use of magnetite NPs and NCs could have potential application as a preventative additive or remedy following failure due to overloading.

To demonstrate the preventive effect of NPs and NCs against overloading, recovered reactors were newly fed with a pulse of glucose (using the same amount initially fed, 6.5 g/L). In this case, no inhibition was observed after the feed (Fig. 2A, New pulse). Biogas production resumed immediately after the pulse without presenting a pronounced lag phase. Methane content in biogas was also in an appropriate range, around 60 %, indicating a non-inhibited process. In this sense, as previously pointed out, the presence of NPs endows the system with certain characteristics that promote microbial activity in relation to substrate degradation, such as increases in surface area, reactivity and the number of active sites (Ellacuriaga et al., 2021). In particular, magnetite NPs are postulated as accelerators of methane production, by favouring the transfer of electrons between the species that supply the compounds required by methanogens (Zhong et al., 2020). Thus, the effect caused by the NPs seems to favour a more adapted and resilient microbial community composition (Lim et al., 2022), able to better withstand further perturbations.

3.3. Recovery of overloaded batch reactors inoculated with flocculent sludge (FS)

Fig. 3A shows methane evolution in the batch test using FS. In this experiment different doses of NPs (from 0.075 g/L to 1 g/L) were studied. As observed in Fig. 3B, reactors supplemented with magnetite NPs recovered from inhibition within 30 and 50 days depending on the dose. Significant differences were observed both in time and biogas production depending on the dose evaluated. The highest dose (1 g/L) showed faster recovery and higher methane production than lower doses. In addition, as observed in Fig. 3B, the dose of 1 g/L after the recovery showed the minimum VFA levels of all samples evaluated. The second highest dose (0.5 g/L) was also effective at recovering the process although more time was needed (around 40 days). VFA reduction was also evident in comparison with control reactors with no NPs. However, only one triplicate reactor of dose 0.25 g/L successfully recovered the process. This replicate also showed a reduction of VFA in Fig. 3B (25_R) whereas the others had the same amount of VFA as the control reactors with no NPs. In fact, lower doses were not effective in the recovery. Different results obtained using the dose of 0.25 g/L indicates the threshold of applicability of this dose according to the level of inhibition. VFA concentrations in experiments inoculated with FS were much higher than the ones observed in experiments using GS, where NPs concentration of 0.27 g/L was effective in the recovery of all inhibited replicates. However, despite the high levels of total VFA found in FS reactors (around 18000 mg/L) the system recovered when NPs were supplemented. As previously indicated, a higher amount of glucose was necessary to inhibit FS reactors (section 2.3). This fact may lead to a high VFA accumulation in reactors without NPs supplementation. Recently, Lim et al. (2022) recovered reactors with similar VFA concentrations via the supplementation of zero valent iron NPs. The effective use of NPs according to the level of inhibition should be carefully addressed to obtain a reliable dose in the recovery of the process. Dosage adjustment has been previously pointed out as a strategy to maintain the positive effects of iron NPs in semicontinuous anaerobic digesters, where higher doses sustained positive effects for a longer time (Barrena et al., 2021).

As observed in this work, the use of magnetite-based nanoparticles allowed for the recovery of the process under conditions of overloading for both GS and FS inoculants. In that sense, the study of the microbial population structure of both inocula before and after the recovery appears interesting to know the applicability of nanomaterials as an additive to correct and prevent process imbalances of different types of anaerobic digesters.

3.4. Effect of process conditions on microbial community: granular sludge

The results derived from the biodiversity analysis for GS (Fig. 4) indicate the loss of diversity in inhibited reactors compared to the control. As observed, the microbiome associated with AD subjected to VFA inhibition was recovered, at least partially, with the incorporation of NPs. Specifically, the alpha diversity values obtained showed the similarity in this respect between the control and the samples supplemented with NPs. Thus, the values found in the GS processes were around 700–800, 500–600 and 4, for CHAO1, number of ASVs and Shannon, respectively, except for the process inhibited, for which the respective levels were 420, 294 and 2.40. These values are similar to those described in literature in relation to the microbial community present at the end of a batch AD (Wang et al., 2021). Slight differences are likely due to the nature of the inoculum and the way the process is operated (Li et al., 2020).

The results from the study of beta diversity also support the hypothesis that the use of NPs in inhibited anaerobic digesters allowed a certain degree of recovery of the microbiome, increasing the similarity of the communities present, both qualitatively and quantitatively, with respect to those associated with non-inhibited processes. Thus, the values found for the Sorensen-Dice index (Fig. 4b) showed higher levels of homology between the final microbiome of the control process and that of the processes with NPs presence compared to the inhibited processes. Microbial homogeneity levels were also increased in presence of the stabilizer (TMAOH), although in in a lower extend than in presence of/with NPs. This lower capacity of the stabilizer to return the microbial community to the population levels of the control may explain to a large extent the non-recovery of the process (in biogas production terms), an aspect discussed in section 3.2. These patterns observed for the different types of AD were repeated both in terms of species identity and relative abundance, although the similarity values were always higher in the first case. This may be a consequence of a redistribution of the relative abundances of species, so that the presence of the NPs favours the development of certain microorganisms over others that, without being inhibited or disappearing, show a lower tolerance to the NPs, as suggested by Eduok et al. (2017).

The analysis performed on the most dominant microbial community members (relative abundance greater than 1 % in at least one of the processes) showed similar conclusions (Fig. 5A) to those described for the entire microbiome (Fig. 4). Thus, the inhibited process was clearly differentiated from the others, all of them grouped in the same cluster, which confirms the recovery action of the NPs. Comparing the relative abundances of the dominant ASVs present in each of the processes, it can be observed how the high addition of glucose decreased both the relative proportion and diversity of methanogens, and intensely enhanced the abundance of representatives of the genus *Clostridium*, especially *C. butyricum*, which reached almost 45 % of the total population. Members of the phylum Firmicutes, practically absent in the control process, were also detected in the processes with the presence of NPs, although the relative abundances found did not exceed 5 % in any case.

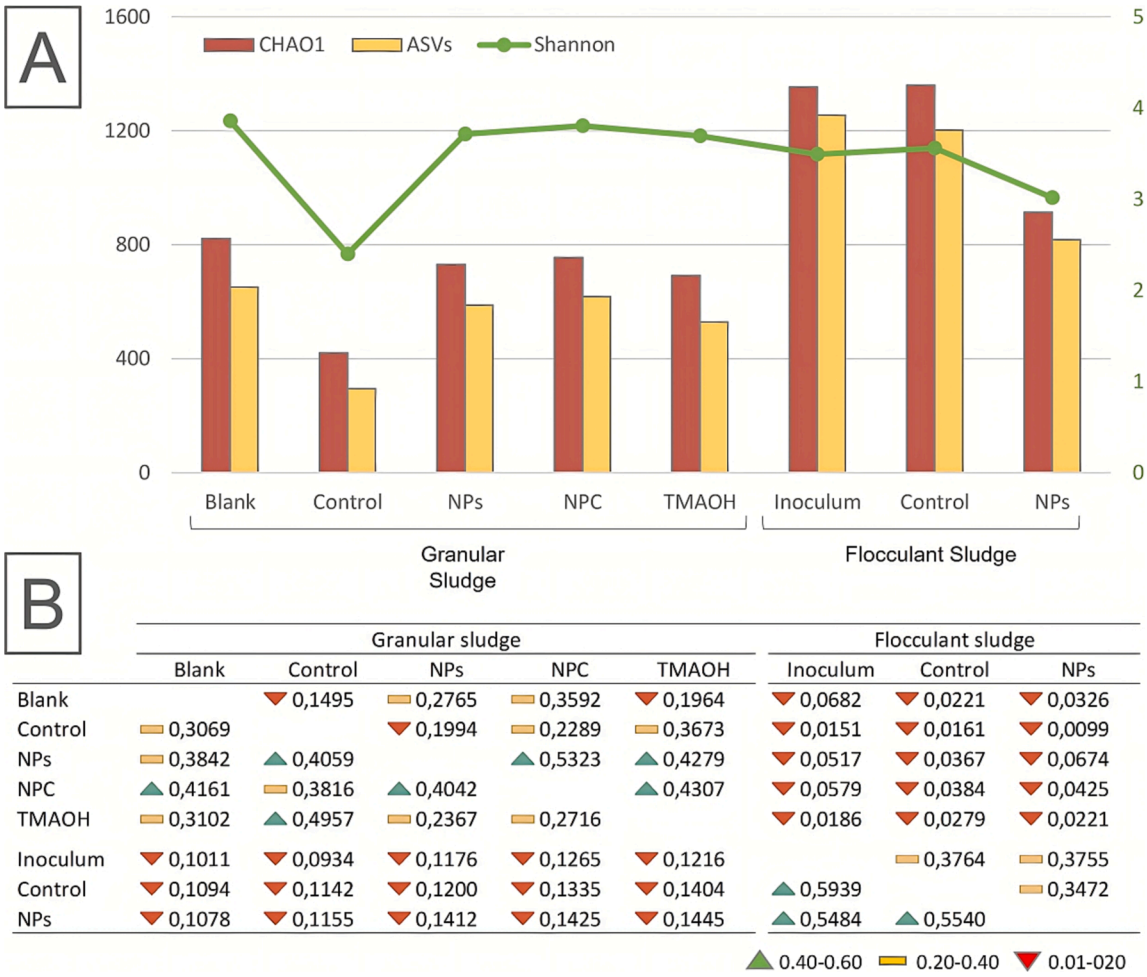

Fig. 4. Diversity indexes found for the different anaerobic digestions analysed; A) Alpha diversity: Chao1, number of ASVs and Shannon; B) Beta diversity: Sorensen-Dice (the qualitative index is shown in the upper diagonal and the quantitative index in the lower diagonal).

Although a specific taxonomic affiliation could not be obtained for several of them, their evolutionary relationships place them in the clostridia group. Many clostridia are characterized as syntrophic acetate oxidizers (Westerholm et al., 2019), capable of providing H_2 and CO_2 to the hydrogenotrophic methanogens (Werner et al., 2014). This is consistent with the redistribution observed in the methanogenic community (Fig. 5A-B), where the dominance of *Methanothrix soehngenii* in the control process, a species widely recognized as an acetoclastic methanogen, was replaced in the NPs-bearing processes by that of *Methanobacterium beijingense*, which produces methane from H_2. The explanation for this effect seems to be related to the ability of some species of *Methanobacterium* to accept electrons directly, an activity recently associated with species of this genus (Zheng et al., 2020), and the stimulus that NPs generates on this ability because of its conductive capability (Vu et al., 2020). This stimulating effect has been observed even in processes with high OLR, as in the present case (Zhao et al., 2017). On the other hand, and although studies in this sense are scarce, it is also necessary to consider the possibility that NPs with conductive behaviour directly affect the activity of methanogenic species, without the intervention of other species (Salvador et al., 2017).

The ability of NPs to partially recover the AD process can be appreciated more directly by studying the entire methanogenic community (Fig. 5B-C), since this is the community most sensitive to the occurrence of disruptive events such as substrate inhibition and VFA accumulation (De Vrieze et al., 2015). It can be seen how the abundance of species belonging to the methanogenic community partially recovered from the drop experienced in the presence of glucose because of the incorporation of NPs. This recovery was especially remarkable in the case of NCs, not only in terms of the percentage of methanogens with respect to the total population, but also in terms of the similarity of both communities, since it was the only case in which the quantitative homology exceeded 50 %, as indicated by the Sorensen-Dice index values (Fig. 5C). In addition to its contribution as an additional conductive material, graphene has been reported to be able to recover processes with high VFA production, characterized by the generation of excessively acidic pH values, not suitable for methanogenic communities (Wu et al., 2020).

On the other hand, the analysis of the entire methanogenic community also explains the lower recovery shown by the process that incorporated the stabilizing agent. In this case, and although the homology with respect to the control process was high (above 87 %) at the level of taxonomic affiliation of the ASVs present, the quantitative distributions of such ASVs in both cases led to a decrease in the observed similarity to values below 43 %. On the contrary, the degree of quantitative homology with respect to the process supplemented with glucose reached a level close to 81 %. In both processes, the dominant methanogens were *Methanobacterium beijingense* and *M. petrolearium*, species that have been reported to be unable to utilize methyl (Ma et al., 2005), or to do so without parallel methane production detected (Mori and Harayama, 2011).

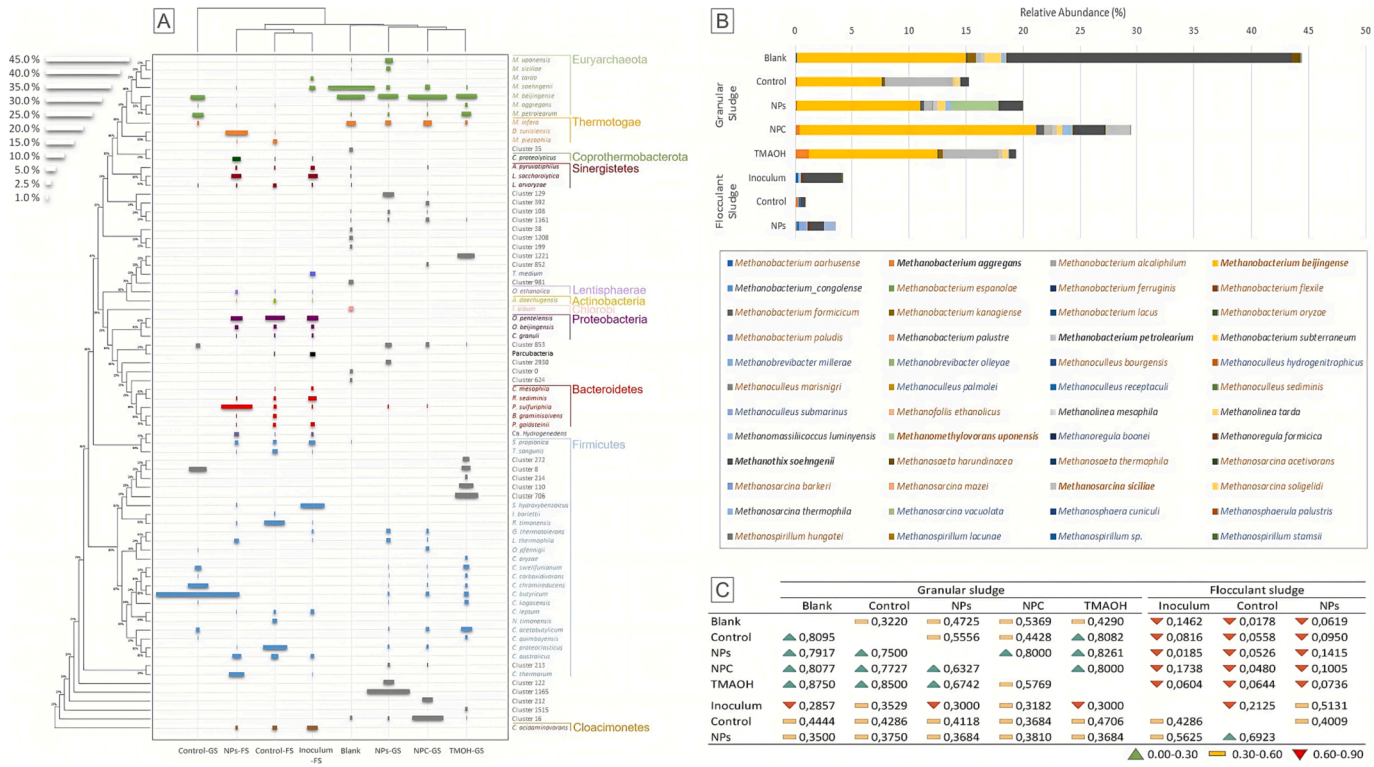

Fig. 5. Analysis of the prokaryotic populations associated with the different anaerobic digestion processes carried out; A) Evolutionary relationships between the species present with relative abundance levels above 1 % in at least one of the processes, relative abundances associated with each of them and dendrogram showing the grouping of the different digestions according to this dominant microbiota; B) Structure of the different methanogenic communities. The legend shows in brown the species associated to the processes with GS, in blue those associated to the processes with FS and in gray the shared ones. Those with relative abundances greater than 1 % are highlighted in bold; C) Sorensen-Dice index for the methanogenic communities Diversity indexes found for the different anaerobic digestions analysed; A) Alpha diversity: Chao1, number of ASVs and Shannon; B) Beta diversity: Sorensen-Dice (the qualitative index is shown in the upper diagonal and the quantitative index in the lower diagonal). (For interpretation of the references to colour in this figure legend, the reader is referred to the web version of this article.)

3.5. Effect of process conditions on microbial community: Flocculent sludge

Inoculum type has been pointed out in numerous studies as the most influential factor for the microbiota of AD processes, even above others such as the inoculum origin or the operating system. Although in the long-term the composition of the microbial community tends to converge (Peces et al., 2018), except for the methanogenic community (Wojcieszak et al., 2017). The results presented herein support the importance that the inoculum has on the composition of the microbial community associated with AD. This is shown by the Sorensen beta diversity index (Fig. 4), for which the values found between processes inoculated with GS and FS did not exceed 15 % and 6 % in any case, in qualitative and quantitative terms, respectively. The microbiome associated with the FS process was characterized by a greater diversity in terms of the number of phyla detected, with the presence of representatives assigned to Proteobacteria, Bacteroidetes and Chloroflexi, barely significant in the case of the GS. According to the literature, these phyla appear to be common in processes seeded with FS (Ribera-Pi et al., 2020). For example, *Ottowia pentelensis*, the major proteobacterium in all three processes, is recognized for its ability to form flocs, which gives it a prominent role in this type of sludge. Moreover, its hydrolytic activity (Feng et al., 2016) allows it to participate in the first stage of the AD process. *Petrimonas sulfuriphila* is also considered a hydrolytic species, with production of acetic acid, H_2 and CO_2. This bacterium of the phylum Bacteroidetes has been detected in relatively high abundance in an AD process amended with magnetite (Ziganshina et al., 2021), as in the present case. Among the representatives of the phylum Chloroflexi, *Levilinea saccharolytica* was the most prominent species. This bacterium seems to have a prominent role in the acidogenic stage of methanogenesis (Sposob et al., 2021), during which it generates H_2 in addition to acetic and lactic acid. This favours the action of both acetogenic and hydrogenotrophic methanogens, as in the case of the process with NPs.

Differences were also manifested in relation to the phylum Firmicutes, important in both types of processes, with dominance of ASVs belonging to the Clostridia group. However, in the GS process most of the ASVs were identified as members of the genus *Clostridium*, contrary to the FS process. In FS process without NPs the dominant species was *Sedimentibacter hydroxybenzoicus*. By comparison, in the FS process with NPs, dominant species were *Calaromator australicus* and, to a greater extent, *Caldalkalibacillus thermarum*, assigned to the phylum Bacilli. *S. hydroxybenzoicus* is associated with the production of acids, especially acetic acid (Klang et al., 2019), which supports the fundamentally acetoclastic behaviour of the control process. *C. thermarum* and *C. australicus*, both thermophilic species, have been previously found in AD systems, the former being able to degrade carbohydrates and VFA (Yan et al., 2020), and the latter, detected in H_2-producing environments, producing acetic acid and ethanol (Mohd Yasin et al., 2011).

When the methanogenic community was considered exclusively, the similarity between processes seeded with different inocula increased slightly, with maximum levels of 48 % and 18 %, respectively (Fig. 5c). However, the response caused by the incorporation of NPs to the inhibited process, concerning the recovery of biogas production capacity, was similar to that described in the case of GS. On this occasion, the recovery seems to be a consequence of the reestablishment of part of the methanogenic species, since it went from 21 % of similarity between the inoculum and the inhibited process, to 51 % detected between the inoculum and the process with added NPs. In fact, the methanogenic community in the inhibited process was practically non-existent,

accounting for<1 % of the total community. *Methanothrix soehngenii*, at 0.32 % relative abundance, was the most abundant methanogenic species. It was also dominant in the other two processes, but the quantified relative abundance was 3.34 % and 1.30 % for the control process and with NPs, respectively. These results apparently differ from those discussed in the case of GS process, where the presence of NPs changed the nature of the methanogenic population from being mostly acetoclastic to being dominated by a hydrogenotrophic species. However, it should be mentioned that the second most abundant species in the methanogenic community of the FS process recovered with NPs was *Methanoculleus submarinus*, a hydrogenotroph (Mikucki et al., 2003), not detected in the control process. The presence of *L. saccharolytica* and, especially, *P. sulfuriphila* in the NPs process, two H_2-producing bacteria, could explain the detection of this methanogen. The low growth rate of the methanogenic community could explain the long recovery times observed in both batch experiments.

3.6. Comparative analysis of the microbial community as a function of the factors under study: SIMPER and Indicator species analyses

Both microbial communities for FS and GS processes were studied in detail. The study involved the initial microbial communities and their evolution following exposure to the nanomaterials. Differences were found between the community at the start and end of the processes. In the case of the initial microbial communities, this was due to the source of the inoculum. After the exposure to nanomaterials, the results were also different. Specifically, the results obtained in relation to the composition of the different microbial communities were studied by applying SIMPER and Indicator Species analyses, which report the percentage contribution of each species to the level of dissimilarity between processes and the identity of the most significant species in each case, respectively. As indicated by the values of the beta diversity indices, the most marked differences in the microbiome were ascribed to the type of inoculum (Fig. 6). The number of species significantly highlighted in terms of type of inoculum was clearly higher than that detected in the case of the presence of NPs and the recovery effect. In the GS process, the statistically dominant microbiota was mostly related to methanogenic species as well as representatives of the genus *Clostridium*, while inoculation with FS resulted in a much more diverse community in terms of the taxonomic affiliation of the significant species. Particularly striking is the non-significance of methanogenic species in the FS process, something already described by other authors, who associate this fact to the concurrence of better conditions for this prokaryotic group in GS (Winkler et al., 2012).

The presence of NPs as a differentiating criterion led to the identification of only one species as significant, *Lutispora thermophila*. This representative of the phylum Firmicutes only appeared at prominent levels in the samples in which NPs were incorporated. This is a species mostly related to amino acid fermentation (Venkiteshwaran et al., 2017), which may point to a possible influence of magnetite NPs on the

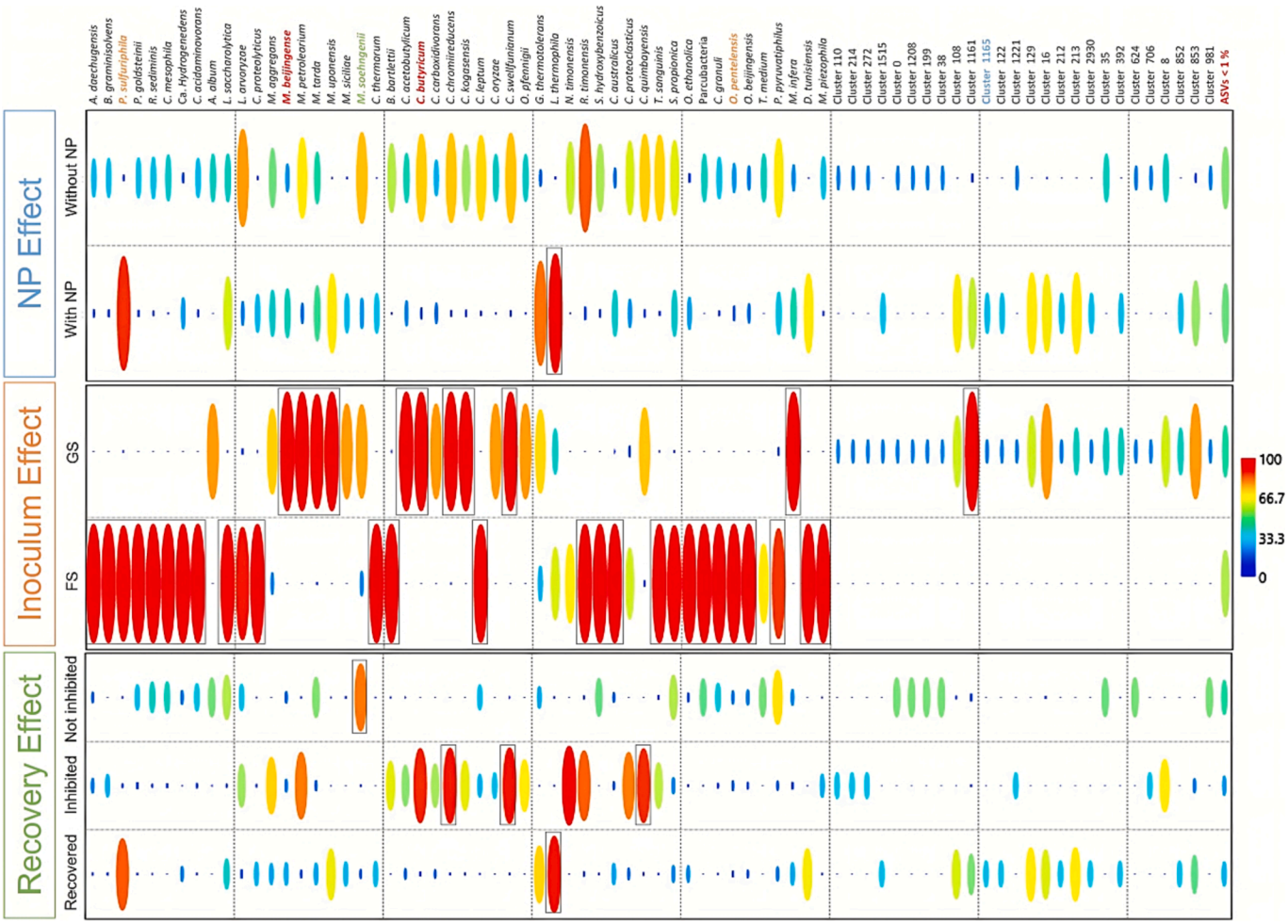

Fig. 6. SIMPER and Indicator Species analyses for species showing relatives abundances higher than 1 % in at least one process, according to addition of NP, inoculum type and recovery effect. Significant species in each case according to Indicator Species analysis have been marked with a rectangle, while major contributors to dissimilarity (>3%) according to SIMPER analysis have been highlighted according to the colour assigned to each specific effect. In red are highlighted those species that contribute in all cases. (For interpretation of the references to colour in this figure legend, the reader is referred to the web version of this article.)

presence of these compounds, as it has already been reported (Li et al., 2019). This same species was also the only one significantly differentiated in the processes operated to recover methanogenic activity, while *Metanothrix soehngenii* was significantly differentiated in the control processes. In the case of the processes inhibited with glucose, three representatives of the Clostridia group stood out statistically with respect to the rest of the species, which is common in processes overloaded with this sugar (Li et al., 2015).

Most of the species cited were those indicated by the SIMPER analysis as the main contributors to the existing dissimilarities between processes grouped according to the aforementioned criteria (Fig. 6). Thus, *Methanobacterium beijingense* and *Clostridium butyricum* were shown to be determinant in differentiating processes, regardless of the criteria adopted. Moreover, Cluster 1165, evolutionarily close to the Clostridia group, *Petrimonas sulfuriphila* and *Ottowia pentelensis*, and *Methanothrix soehngenii* were for NPs, type of inoculum, and recovery effects, respectively.

4. Conclusions

Anaerobic digestion supplemented with magnetite-based NPs could be an effective strategy to operate at high OLR improving the stability of the AD. NPs addition shows the ability to recover the microbiome associated with AD subjected to VFA inhibition, especially the reestablishment of the methanogenic communities but also changing the dominance favouring hydrogenotrophic species (*Methanobacterium beijingense*). Species related to amino acid fermentation (*Lutispora thermophila)* appear as the most differentiating criteria related to NPs presence, regardless the starting inoculum. Further experiments in continuous conditions should be addressed to gain knowledge about both effective operational use of NPs and economics of the process.

CRediT authorship contribution statement

Raquel Barrena: Conceptualization, Investigation, Visualization, Writing – original draft. **María del Carmen Vargas-García:** Formal analysis, Visualization, Writing – original draft. **Paula Catacora-Padilla:** Investigation, Validation. **Teresa Gea:** Validation, Writing – review & editing. **Ahmad Abo Markeb:** Resources. **Javier Moral-Vico:** Resources, Writing – original draft. **Antoni Sánchez:** Writing – review & editing. **Xavier Font:** Conceptualization, Writing – review & editing. **Thomas J. Aspray:** Conceptualization, Supervision, Writing – review & editing.

Declaration of Competing Interest

The authors declare that they have no known competing financial interests or personal relationships that could have appeared to influence the work reported in this paper.

Data availability

Data will be made available on request.

Acknowledgments

Raquel Barrena is grateful to TECNIOspring fellowship programme (TECSPR15-1-0051) co-financed by the European Union through the Marie Curie Actions and ACCIÓ (Generalitat de Catalunya).

As Antoni Sánchez, a [co-]author on this paper, is an editorial board member of Bioresource Technology, he was blinded to this paper during review, and the paper was independently handled by Samir Kumar Khanal as editor.

Appendix A. Supplementary data

Supplementary data to this article can be found online at https://doi.org/10.1016/j.biortech.2023.128632.

References

Abo Markeb, A., Llimós-Turet, J., Ferrer, I., Blánquez, P., Alonso, A., Sánchez, A., Moral-Vico, J., Font, X., 2019. The use of magnetic iron oxide based nanoparticles to improve microalgae harvesting in real wastewater. Water Res. 159, 490–500. https://doi.org/10.1016/j.watres.2019.05.023.

Angelidaki, I., Boe, K., Ellegaard, L., 2005. Effect of operating conditions and reactor configuration on efficiency of full-scale biogas plants. Water Sci. Technol. a J. Int. Assoc. Water Pollut. Res. 52, 189–194.

Arif, S., Liaquat, R., Adil, M., 2018. Applications of materials as additives in anaerobic digestion technology. Renew. Sustain. Energy Rev. 97, 354–366. https://doi.org/10.1016/j.rser.2018.08.039.

Barrena, R., Vargas-García, M.D.C., Capell, G., Barańska, M., Puntes, V., Moral-Vico, J., Sánchez, A., Font, X., 2021. Sustained effect of zero-valent iron nanoparticles under semi-continuous anaerobic digestion of sewage sludge: Evolution of nanoparticles and microbial community dynamics. Sci. Total Environ. 777 https://doi.org/10.1016/j.scitotenv.2021.145969.

Cai, W., Wan, J., 2007. Facile synthesis of superparamagnetic magnetite nanoparticles in liquid polyols. J. Colloid Interface Sci. 305, 366–370. https://doi.org/10.1016/j.jcis.2006.10.023.

Casals, E., Barrena, R., García, A., González, E., Delgado, L., Busquets-Fité, M., Font, X., Arbiol, J., Glatzel, P., Kvashnina, K., Sánchez, A., Puntes, V., 2014. Programmed iron oxide nanoparticles disintegration in anaerobic digesters boosts biogas production. Small 10 (14), 2801–2808.

Commission, E., Communication, D.-G. for, 2021. Delivering the Green Deal : the role of clean gases including hydrogen. Publications Office of the European Union. doi/10.2775/718801.

Daraei, H., Rafiee, M., Yazdanbakhsh, A.R., Amoozegar, M.A., Guanglei, Q., 2019. A comparative study on the toxicity of nano zero valent iron (nZVI) on aerobic granular sludge and flocculent activated sludge: Reactor performance, microbial behavior, and mechanism of toxicity. Process Saf. Environ. Prot. 129, 238–248. https://doi.org/10.1016/j.psep.2019.07.011.

De Vrieze, J., Gildemyn, S., Vilchez-Vargas, R., Jáuregui, R., Pieper, D.H., Verstraete, W., Boon, N., 2015. Inoculum selection is crucial to ensure operational stability in anaerobic digestion. Appl. Microbiol. Biotechnol. 99, 189–199. https://doi.org/10.1007/s00253-014-6046-3.

Eduok, S., Ferguson, R., Jefferson, B., Villa, R., Coulon, F., 2017. Aged-engineered nanoparticles effect on sludge anaerobic digestion performance and associated microbial communities. Sci. Total Environ. 609, 232–241. doi: 10.1016/j.scitotenv.2017.07.178.

Ellacuriaga, M., Cascallana, J.G., González, R., Gómez, X., 2021. High-solid anaerobic digestion: reviewing strategies for increasing reactor performance. Environ. – MDPI 8 (8), 80.

Feng, Q., Song, Y.C., Bae, B.U., 2016. Influence of applied voltage on the performance of bioelectrochemical anaerobic digestion of sewage sludge and planktonic microbial communities at ambient temperature. Bioresour. Technol. 220, 500–508. https://doi.org/10.1016/j.biortech.2016.08.085.

Holliger, C., Alves, M., Andrade, D., et al., 2016. Towards a standardization of biomethane potential tests. Water Sci. Technol. 74, 2515–2522. doi: 10.2166/wst.2016.336.

Klang, J., Szewzyk, U., Bock, D., Theuerl, S., 2019. Nexus between the microbial diversity level and the stress tolerance within the biogas process. Anaerobe 56, 8–16. https://doi.org/10.1016/j.anaerobe.2019.01.003.

Kong, X., Yu, S., Fang, W., Liu, J., Li, H., 2018. Enhancing syntrophic associations among Clostridium butyricum, Syntrophomonas and two types of methanogen by zero valent iron in an anaerobic assay with a high organic loading. Bioresour. Technol. 257, 181–191. https://doi.org/10.1016/j.biortech.2018.02.088.

Lee, J., Koo, T., Yulisa, A., Hwang, S., 2019. Magnetite as an enhancer in methanogenic degradation of volatile fatty acids under ammonia-stressed condition. J. Environ. Manage. 241, 418–426. https://doi.org/10.1016/j.jenvman.2019.04.038.

Li, Y.F., Abraham, C., Nelson, M.C., Chen, P.H., Graf, J., Yu, Z., 2015. Effect of organic loading on the microbiota in a temperature-phased anaerobic digestion (TPAD) system co-digesting dairy manure and waste whey. Appl. Microbiol. Biotechnol. 99, 8777–8792. https://doi.org/10.1007/s00253-015-6738-3.

Li, S., Cao, Y., Zhao, Z., Zhang, Y., 2019. Regulating secretion of extracellular polymeric substances through dosing magnetite and zerovalent iron nanoparticles to affect anaerobic digestion mode. ACS Sustain. Chem. Eng. 7, 9655–9662. https://doi.org/10.1021/acssuschemeng.9b01252.

Li, S., Li, D., Wang, Y., Zeng, H., Yuan, Y., Zhang, J., 2020. Startup and stable operation of advanced continuous flow reactor and the changes of microbial communities in aerobic granular sludge. Chemosphere 243, 125434. https://doi.org/10.1016/j.chemosphere.2019.125434.

Lim, E.Y., Lee, J.T.E., Zhang, L., Tian, H., Ong, K.C., Tio, Z.K., Zhang, J., Tong, Y.W., 2022. Abrogating the inhibitory effects of volatile fatty acids and ammonia in overloaded food waste anaerobic digesters via the supplementation of nano-zero valent iron modified biochar. Sci. Total Environ. 817, 152968 https://doi.org/10.1016/j.scitotenv.2022.152968.

Ma, K., Liu, X., Dong, X., 2005. Methanobacterium beijingense sp. nov., a novel methanogen isolated from anaerobic digesters. Int. J. Syst. Evol. Microbiol. 55, 325–329. https://doi.org/10.1099/ijs.0.63254-0.

Ma, K., Wang, W., Liu, Y., Bao, L., Cui, Y., Kang, W., Wu, Q., Xin, X., 2021. Insight into the performance and microbial community profiles of magnetite-amended anaerobic digestion: varying promotion effects at increased loads. Bioresour. Technol. 329, 124928 https://doi.org/10.1016/j.biortech.2021.124928.

Mikucki, J.A., Liu, Y., Delwiche, M., Colwell, F.S., Boone, D.R., 2003. Isolation of a methanogen from deep marine sediments that contain methane hydrates, and description of Methanoculleus submarinus sp. nov. Appl. Environ. Microbiol. 69, 3311–3316. https://doi.org/10.1128/AEM.69.6.3311-3316.2003.

Mohd Yasin, N.H., Rahman, N.A., Man, H.C., Mohd Yusoff, M.Z., Hassan, M.A., 2011. Microbial characterization of hydrogen-producing bacteria in fermented food waste at different pH values. Int. J. Hydrogen Energy 36, 9571–9580. https://doi.org/10.1016/j.ijhydene.2011.05.048.

Mori, K., Harayama, S., 2011. Methanobacterium petrolearium sp. nov. and Methanobacterium ferruginis sp. nov., mesophilic methanogens isolated from salty environments. Int. J. Syst. Evol. Microbiol. 61, 138–143. https://doi.org/10.1099/ijs.0.022723-0.

Peces, M., Astals, S., Jensen, P.D., Clarke, W.P., 2018. Deterministic mechanisms define the long-term anaerobic digestion microbiome and its functionality regardless of the initial microbial community. Water Res. 141, 366–376. https://doi.org/10.1016/j.watres.2018.05.028.

Ribera-Pi, J., Campitelli, A., Badia-Fabregat, M., Jubany, I., Martínez-Lladó, X., McAdam, E., Jefferson, B., Soares, A., 2020. Hydrolysis and Methanogenesis in UASB-AnMBR treating municipal wastewater under psychrophilic conditions: importance of reactor configuration and inoculum. Front. Bioeng. Biotechnol. doi: 10.3389/fbioe.2020.567695.

Salama, A.M., Abedin, R.M.A., Elwakeel, K.Z., 2021. Influences of greenly synthesized iron oxide nanoparticles on the bioremediation of dairy effluent using selected microbial isolates. Int. J. Environ. Sci. Technol. 19, 7019–7030. https://doi.org/10.1007/s13762-021-03625-3.

Salvador, A.F., Martins, G., Melle-Franco, M., Serpa, R., Stams, A.J.M., Cavaleiro, A.J., Pereira, M.A., Alves, M.M., 2017. Carbon nanotubes accelerate methane production in pure cultures of methanogens and in a syntrophic coculture. Environ. Microbiol. 19 (7), 2727–2739.

Siegert, I., Banks, C., 2005. The effect of volatile fatty acid additions on the anaerobic digestion of cellulose and glucose in batch reactors. Process Biochem. 40, 3412–3418. https://doi.org/10.1016/j.procbio.2005.01.025.

Sposob, M., Moon, H.-S., Lee, D., Yun, Y.-M., 2021. Microbiome of seven full-scale anaerobic digestion plants in south korea: Effect of feedstock and operational parameters. Energies 14 (3), 665.

Sun, Z., Feng, L., Li, Y., Han, Y., Zhou, H., Pan, J., 2022. The role of electrochemical properties of biochar to promote methane production in anaerobic digestion. J. Clean. Prod. 362, 132296 https://doi.org/10.1016/j.jclepro.2022.132296.

Venkiteshwaran, K., Milferstedt, K., Hamelin, J., Fujimoto, M., Johnson, M., Zitomer, D. H., 2017. Correlating methane production to microbiota in anaerobic digesters fed synthetic wastewater. Water Res. 110, 161–169. https://doi.org/10.1016/j.watres.2016.12.010.

Vu, M.T., Noori, M.T., Min, B., 2020. Conductive magnetite nanoparticles trigger syntrophic methane production in single chamber microbial electrochemical systems. Bioresour. Technol. 296, 122265 https://doi.org/10.1016/j.biortech.2019.122265.

Wang, S., Chen, L., Yang, H., Liu, Z., 2021. Influence of zinc oxide nanoparticles on anaerobic digestion of waste activated sludge and microbial communities. RSC Adv 11 (10), 5580–5589.

Werner, J.J., Garcia, M.L., Perkins, S.D., Yarasheski, K.E., Smith, S.R., Muegge, B.D., Stadermann, F.J., DeRito, C.M., Floss, C., Madsen, E.L., Gordon, J.I., Angenent, L.T., Spormann, A.M., 2014. Microbial community dynamics and stability during an ammonia-induced shift to syntrophic acetate oxidation. Appl. Environ. Microbiol. 80 (11), 3375–3383.

Westerholm, M., Dolfing, J., Schnürer, A., 2019. Growth characteristics and thermodynamics of syntrophic acetate oxidizers. Environ. Sci. Technol. 53, 5512–5520. https://doi.org/10.1021/acs.est.9b00288.

Winkler, M.K.H., Kleerebezem, R., Khunjar, W.O., de Bruin, B., van Loosdrecht, M.C.M., 2012. Evaluating the solid retention time of bacteria in flocculent and granular sludge. Water Res. 46, 4973–4980. https://doi.org/10.1016/j.watres.2012.06.027.

Wojcieszak, M., Pyzik, A., Poszytek, K., Krawczyk, P.S., Sobczak, A., Lipinski, L., Roubinek, O., Palige, J., Sklodowska, A., Drewniak, L., 2017. Adaptation of methanogenic inocula to anaerobic digestion of maize silage. Front. Microbiol. https://doi.org/10.3389/fmicb.2017.01881.

Wu, B., Lin, R., Kang, X., Deng, C., Xia, A., Dobson, A.D.W., Murphy, J.D., 2020. Graphene addition to digestion of thin stillage can alleviate acidic shock and improve biomethane production. ACS Sustain. Chem. Eng. 8, 13248–13260. https://doi.org/10.1021/acssuschemeng.0c03484.

Yan, M., Fotidis, I.A., Jéglot, A., Treu, L., Tian, H., Palomo, A., Zhu, X., Angelidaki, I., 2020. Long-term preserved and rapidly revived methanogenic cultures: Microbial dynamics and preservation mechanisms. J. Clean. Prod. 263 https://doi.org/10.1016/j.jclepro.2020.121577.

Yan, W., Shen, N., Xiao, Y., Chen, Y., Sun, F., Kumar Tyagi, V., Zhou, Y., 2017. The role of conductive materials in the start-up period of thermophilic anaerobic system. Bioresour. Technol. 239, 336–344. https://doi.org/10.1016/J.BIORTECH.2017.05.046.

Zhang, Z., Guo, L., Wang, Y., Zhao, Y., She, Z., Gao, M., Guo, Y., 2020. Application of iron oxide (Fe3O4) nanoparticles during the two-stage anaerobic digestion with waste sludge: Impact on the biogas production and the substrate metabolism. Renew. Energy 146, 2724–2735. https://doi.org/10.1016/j.renene.2019.08.078.

Zhang, J., Zhao, W., Zhang, H., Wang, Z., Fan, C., Zang, L., 2018. Recent achievements in enhancing anaerobic digestion with carbon- based functional materials. Bioresour. Technol. 266, 555–567.

Zhao, Z., Li, Y., Quan, X., Zhang, Y., 2017. Towards engineering application: Potential mechanism for enhancing anaerobic digestion of complex organic waste with different types of conductive materials. Water Res. 115, 266–277. https://doi.org/10.1016/j.watres.2017.02.067.

Zheng, S., Liu, F., Wang, B., Zhang, Y., Lovley, D.R., 2020. Methanobacterium capable of direct interspecies electron transfer. Environ. Sci. Technol. 54, 15347–15354. https://doi.org/10.1021/acs.est.0c05525.

Zhong, D., Li, J., Ma, W., Qian, F., 2020. Clarifying the synergetic effect of magnetite nanoparticles in the methane production process. Environ. Sci. Pollut. Res. 27, 17054–17062. https://doi.org/10.1007/s11356-020-07828-y.

Ziganshina, E.E., Belostotskiy, D.E., Bulynina, S.S., Ziganshin, A.M., 2021. Effect of magnetite on anaerobic digestion of distillers grains and beet pulp: Operation of reactors and microbial community dynamics. J. Biosci. Bioeng. 131, 290–298. https://doi.org/10.1016/j.jbiosc.2020.10.003.